Inelastic cross sections in Cs($n\,^2D_J$) + Cs($6\,^2S_{1/2}$) collisions

A. C. Tam,* T. Yabuzaki,† S. M. Curry,‡ M. Hou, and W. Happer
Columbia Radiation Laboratory, Physics Department, Columbia University, New York, New York 10027
(Received 27 December 1977)

The inelastic collisional cross sections of the nD states of Cs are measured by the technique of selective laser excitation and observation of collision-induced fluorescence. The cross sections (in units of 10^{-14} cm^2) for the fine-structure-changing collisions [i.e., Cs($n\,^2D_{3/2}$) + Cs($6\,^2S_{1/2}$)→Cs($n\,^2D_{5/2}$) + Cs($6\,^2S_{1/2}$)] for n being 6–10 are 2.7 ± 0.5, 3.7 ± 0.7, 8.6 ± 1.7, 18.4 ± 3.7, and 29.8 ± 6.0, respectively. The cross sections (in 10^{-14} cm^2) for excitation transfer out of the nD doublet [i.e., Cs($n\,^2D_{5/2}$) + Cs($6\,^2S_{1/2}$)→states other than Cs(nD)] for n being 6–10 are 1.1 ± 0.6, 5.3 ± 1.5, 3.6 ± 1.5, 6.3 ± 2.3, and 15.5 ± 4.0, respectively. The fine-structure-changing cross sections are found to be nearly equal to the geometrical cross section $\pi n^{*4} a_0^2$ for all the nD states studied, except $6D$, whose fine-structure-changing cross section is unusually large.

I. INTRODUCTION

Many experiments[1–4] and theories[5–8] have been done to study the transfer between the fine-structure levels of the low-lying P states of the alkali-metal atoms owing to collisions with another atom; for example,

$$\mathrm{Cs}(6P_{1/2}) + X \rightleftarrows \mathrm{Cs}(6P_{3/2}) + X\,, \tag{1}$$

where X can be a Cs ground-state atom, or a foreign-gas atom or a molecule like Ne, H_2, N_2, etc. Such experiments have been done both in vapor cells[1–3] and in flames.[4] Recently, collisional transfers involving alkali-metal Rydberg states using selective laser excitations have also been studied.[9,10] These collisional excitation transfers are of interest[11] because such inelastic collisions cause energy redistributions in an excited medium (e.g., in flames, electrically excited discharges, and optically pumped systems) and modify the physical and chemical properties of the medium. Also, experimental values of such excitation-transfer cross sections provide critical tests of computed interatomic potential curves.[12] Until now, excitation-transfer collisions of the type given in (1) have been studied only for P states of alkali-metal atoms. The present study seems to be the first experimental investigation of the fine-structure-changing collisional cross section of alkali-metal nD states. The collisional partner is the alkali ground state in the present investigation. We have measured the cross sections for the following inelastic collisions for $n = 6 - 10$:

$$\mathrm{Cs}(nD_{5/2}) + \mathrm{Cs}(6S) \underset{\sigma'_{fs}}{\overset{\sigma_{fs}}{\rightleftarrows}} \mathrm{Cs}(nD_{3/2}) + \mathrm{Cs}(6S) \tag{2}$$

and

$$\mathrm{Cs}(nD_{5/2}) + \mathrm{Cs}(6S) \xrightarrow{\sigma_{tr}} \mathrm{Cs\ states\ other\ than\ Cs}(nD)\,. \tag{3}$$

Here σ_{fs}, σ'_{fs} are fine-structure-changing cross sections, related by the principle of detailed balancing:

$$\sigma_{fs}/\sigma'_{fs} = \exp(E_{fs}/kT)\, g(nD_{3/2})/g(nD_{5/2})\,, \tag{4}$$

where E_{fs} is the fine-structure separation, and the g's are statistical weights. The Boltzmann factor $\exp(E_{fs}/kT)$ is ≈ 1 in the present experiment. In (3), σ_{tr} is the total cross section for transfer out of the nD doublet, with the production of atoms in other states [for example, two Cs($6P$) atoms[13]]. We find that for $n \leq 10$, both σ_{fs} and σ_{tr} are typically of the order of the geometrical cross section $\pi(n^*)^4 a_0^2$ of the excited cesium atom Cs(nD). Here n^* is the effective quantum number of the excited state [see Eq. (11)] and a_0 is the Bohr radius.

II. EXPERIMENT

Our experimental arrangement is illustrated schematically in Fig. 1(a). The experimental cell (3 cm diameter and 7 cm long) was made of aluminosilicate glass (Corning 1720), which proves to be perfectly resistant to corrosion by cesium at temperatures as high as 500 °C. The cell was first evacuated and baked at 650 °C with a vacuum of 10^{-6} torr for a day, and then a little cesium metal from a break-seal ampoule was distilled into it before seal off. The cell is seated in a glass oven and heated to a temperature between 140 °C and 260 °C. The cell temperature is measured by a thermocouple attached to the coolest point of the cell where Cs metal condenses. The observation window is kept about 10 °C hotter than the coolest point of the cell. The laser output from a cw dye laser (Spectra Physics model 580, pumped by a krypton or argon ion laser, depending on the dye used) is focused into the cell, and the fluorescence is dispersed by a 0.3-m monochromator (McPherson model 218), and detected

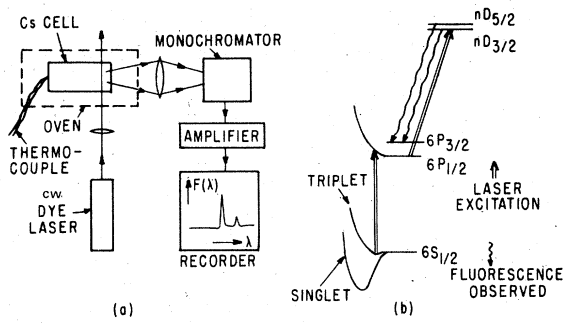

FIG. 1. (a) Schematic diagram of the experimental arrangement. See Table I for details about the cw dye laser. (b) Schematic diagram of the laser excitations and fluorescence observations. The first-step Cs_2 excitation can be a dissociative triplet excitation, a dissociative singlet excitation, or a bound-bound singlet excitation, with relative efficiencies depending on the laser wavelength; the first case is indicated in the figure.

by a refrigerated photomultiplier tube (S-1 or S-20, depending on the wavelength range). At lower temperatures, the observed fluorescence consists mainly of radiation from the particular $n\,^2D_J$ doublet excited by the laser plus fluorescence from the $6P$ doublet; fluorescence from other states is orders of magnitude weaker. The experimental parameters for the various nD states studied ($n = 6$–10) are listed in Table I.

The dye-laser beam populates the $nD_{3/2}$ state by a stepwise excitation process. The dye laser first populates the Cs($6P$) state by exciting the Cs_2 ground-state molecules[13-15] (singlets or triplets); various molecular excited states Cs_2* can be produced by various laser wavelengths. If the Cs_2* is dissociative, it can produce Cs($6P$) atoms by dissociation [as shown in Fig. 1(b) for the case of excitation of triplet ground-state molecules]; if the Cs_2* is bound, it can also produce Cs($6P$) atoms by collisions[16,17]:

$$Cs_2^* + Cs(6S) \rightarrow Cs_2 + Cs(6P). \qquad (5)$$

The cross section for reaction (5) is expected[16,17] to be $\sim 10^{-14}$ cm^2 for nearly resonant collisions. The Cs($6P_{1/2}$) atoms so produced are then excited to the Cs($nD_{3/2}$) by the laser, as indicated in Table I.

Although only Cs($nD_{3/2}$) is produced by the laser, fluorescence from both Cs($nD_{3/2}$) and Cs($nD_{5/2}$) is observed, as shown in Fig. 2. We note that there is no interference from scattered laser light (except for the $n = 10$ case), as excitation is from the Cs($6P_{1/2}$) state while fluorescence to the Cs($6P_{3/2}$) state is detected. For the $n = 10$ case, the limited tuning range of the R6G dye laser forces us to excite the Cs($10D_{3/2}$) state from the Cs($6P_{3/2}$) state, and then instrumental scattering must be carefully minimized, and the monochromator bandwidth must be sufficiently reduced so that we can distinguish one of the fluorescence lines at 5635.2 Å from the scattered laser light at 5636.7 Å (see Table I). The ratio of the fluorescence from Cs($nD_{3/2}$) to that from Cs($nD_{5/2}$) decreases

TABLE I. Experimental parameters to study the various Cs(nD) states.

Excitation transition	Dye-laser wavelength (Å)	Dye-laser characteristics	Typical dye-laser output (mW)	Observed fluorescence transitions	Observed fluorescence wavelengths (Å)
$6P_{1/2} \rightarrow 6D_{3/2}$	8761.4	HITC dye pumped by 5-W red output from a Kr^+ laser	200 (0.5-Å bandwidth)	$6D_{3/2} \rightarrow 6P_{3/2}$	9208.5
				$6D_{5/2} \rightarrow 6P_{3/2}$	9172.3
$6P_{1/2} \rightarrow 7D_{3/2}$	6723.3	Cresyl violet dye pumped by 3-W yellow-green output from a Kr^+ laser	50 (0.5-Å bandwidth)	$7D_{3/2} \rightarrow 6P_{3/2}$	6983.5
				$7D_{5/2} \rightarrow 6P_{3/2}$	6973.3
$6P_{1/2} \rightarrow 8D_{3/2}$	6010.5	R6G dye pumped by 1.7-W green output from an Ar^+ laser	180 (single mode)	$8D_{3/2} \rightarrow 6P_{3/2}$	6217.6
				$8D_{5/2} \rightarrow 6P_{3/2}$	6213.1
$6P_{1/2} \rightarrow 9D_{3/2}$	5664.0	Same	160 (single mode)	$9D_{3/2} \rightarrow 6P_{3/2}$	5847.6
				$9D_{5/2} \rightarrow 6P_{3/2}$	5845.1
$6P_{3/2} \rightarrow 10D_{3/2}$	5636.7	Same	150 (single mode)	$10D_{3/2} \rightarrow 6P_{1/2}$	5465.9
				$10D_{5/2} \rightarrow 6P_{3/2}$	5635.2

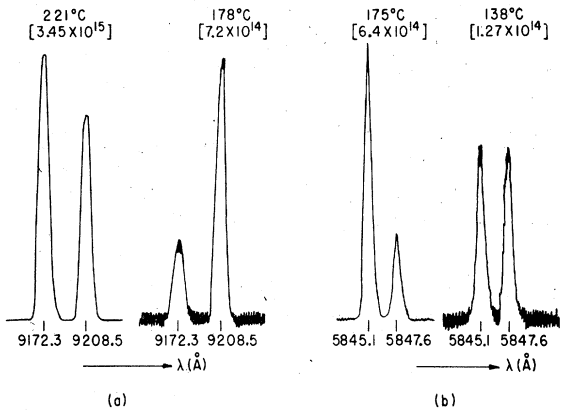

FIG. 2. Typical fluorescence spectra for laser wavelengths being (a) 8761.4 Å ($6D_{3/2}$ populated by laser); and (b) 5664.0 Å ($9D_{3/2}$ populated by laser). For each laser wavelength, the fluorescence spectra for a low cell temperature and for a high cell temperature are given. Cell temperature and the corresponding Cs density in atoms/cm^3 are indicated.

as the temperature increases (see Fig. 2), because as the density of ground-state cesium atoms increases, more Cs($nD_{5/2}$) atoms are produced by collisions [the inverse of reaction (2)]. The ratio of the intensities of the two fluorescence lines for each nD doublet is found to be independent of the laser power, although the intensity of each line increases as the laser power increases. By measuring the ratio of the fluorescence lines as a function of cell temperature (and hence the Cs density), the inelastic-collision cross sections σ_{fs}, σ'_{fs}, and σ_{tr} can be found, as described in III.

III. DATA ANALYSIS

Consider the production rate and loss rate of the Cs($nD_{5/2}$) atoms. They are produced due to fine-structure-changing collisions of Cs($nD_{3/2}$) with ground-state cesium atoms [the inverse of reaction (2)], and they are lost by radiative decays, by fine-structure-changing collisions [forward reaction of Eq. (2)] and by collisional transfers out of the nD doublet [reaction (3)]. In steady state, the production rate and the loss rate are equal; hence

$$N_{3/2}Nv\sigma'_{fs} = N_{5/2}(1/\tau + Nv\sigma_{fs} + Nv\sigma_{tr}), \tag{6}$$

where $N_{3/2}$, $N_{5/2}$, and N are the $nD_{3/2}$, $nD_{5/2}$, and ground-state densities, respectively; v is the average relative atomic velocity; and τ is the radiative lifetime of the $nD_{5/2}$ state. Equation (6) can be rearranged to obtain

$$\frac{N_{3/2}}{N_{5/2}} = \frac{1}{\tau\sigma'_{fs}}\left(\frac{1}{Nv}\right) + \frac{\sigma_{fs}+\sigma_{tr}}{\sigma'_{fs}}. \tag{7}$$

Equation (7) indicates that if $N_{3/2}/N_{5/2}$ is plotted against $(Nv)^{-1}$, a straight line should be obtained and the unknown σ'_{fs} and σ_{tr} can be obtained from the gradient and the intercept. Note that σ'_{fs} and σ_{fs} are related by Eq. (4). The ratio $N_{3/2}/N_{5/2}$ can be obtained from the ratio of the intensities of the fluorescence lines (listed in Table I) by

$$N_{3/2}/N_{5/2} = F_{3/2}A_{5/2}/F_{5/2}A_{3/2}, \tag{8}$$

where $F_{3/2}$, $F_{5/2}$ are the fluorescence intensities observed, and $A_{3/2}$, $A_{5/2}$ are the transition rates (or Einstein A coefficients) of the observed branches from the $nD_{3/2}$, $nD_{5/2}$ states, respectively. No experimental measurements of $A_{3/2}$ and $A_{5/2}$ are known to us; however, several calculations[18-21] of these rates (or the related oscillator strengths) are available. The magnitudes of the transition rates vary substantially among the various authors[18-21]; fortunately, the ratios $A_{5/2}/A_{3/2}$ according to the various calculations[18-21] for each of the nD doublets we studied are nearly constant (typically within ±5%). We shall use the computed values of $A_{5/2}/A_{3/2}$ calculated by Tsekeris and Happer,[18] as listed in Table II, to convert the fluorescence intensity ratios (which are the raw data measured from spectra exemplified in Fig. 2) into population ratios according to Eq. (8). We believe that the $A_{5/2}/A_{3/2}$ ratios listed in Table II are accurate to ± 5%.

The fluorescence intensities $F_{3/2}$ and $F_{5/2}$ are measured as a function of the Cs cell temperature, which can be converted to the Cs density N using Nesmeyanov's formula.[22] Hence, using Eq. (8), we can obtain the ratio $N_{3/2}/N_{5/2}$ as a function of $(Nv)^{-1}$, as plotted in Fig. 3. We see that for each nD state, the experimental points can be fitted by a straight line very well (except for the higher-temperature points for the higher-D states, where complications due to collisions of the D states with

TABLE II. Theoretical transition rates [a] $A_{5/2}$ and $A_{3/2}$ of the observed transitions (listed in Table I) from the Cs($nD_{5/2}$) and Cs($nD_{3/2}$), respectively. The ratio $A_{5/2}/A_{3/2}$ used in Eq. (8) and value of n^* according to Eq. (11) are also listed for the various nD states.

n	$A_{5/2}$ (10^6 sec^{-1})	$A_{3/2}$ (10^6 sec^{-1})	$A_{5/2}/A_{3/2}$	n^*
6	16.3	2.84	5.76	3.54
7	9.58	1.61	5.93	4.53
8	5.82	0.984	5.92	5.53
9	3.84	0.646	5.93	6.53
10	2.67	2.30 [b]	1.157	7.53

[a] According to Tsekeris and Happer (Ref. 18).

[b] Note that the final state for this transition (listed in Table I) is the $6P_{1/2}$ state, while in all the other cases, it is the $6P_{3/2}$ state.

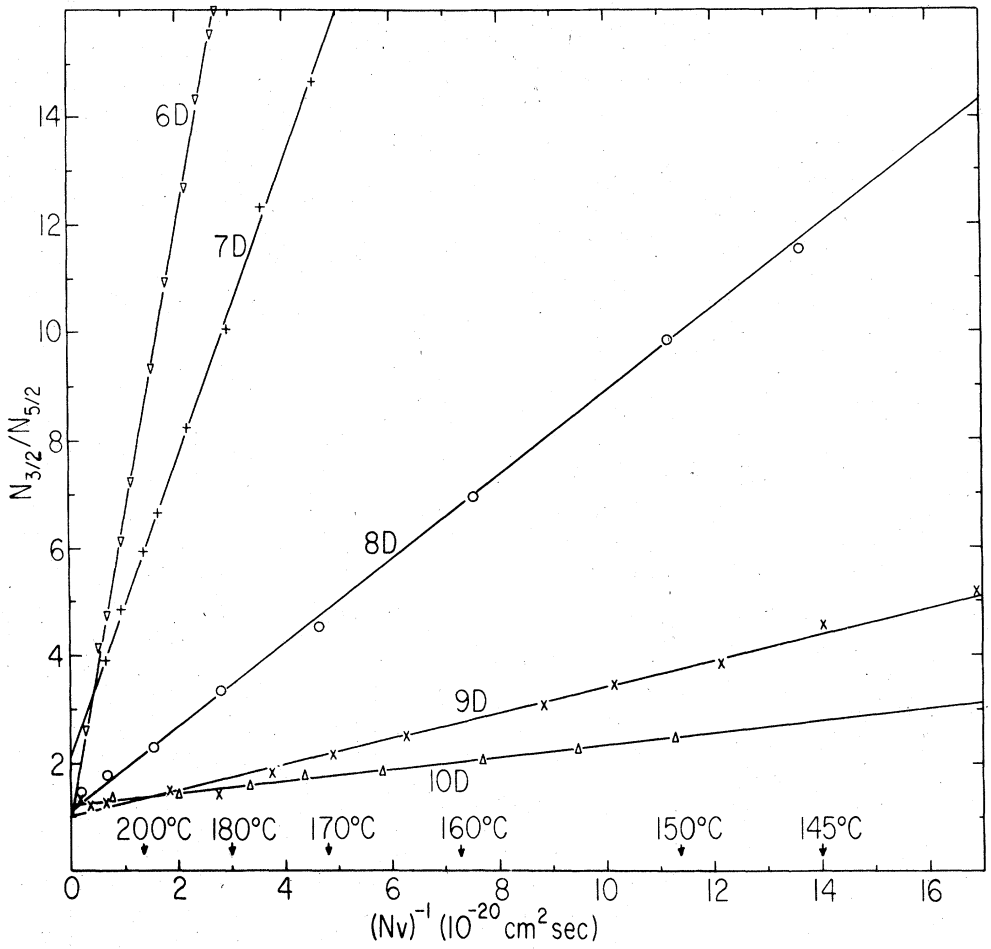

FIG. 3. Plot of the observed population ratio $N_{3/2}/N_{5/2}$ against $(Nv)^{-1}$ for all the Cs(nD) states studied. Cell temperatures are also indicated on the horizontal axis.

Cs($6P$) atoms may be important). The gradient of the fitted straight line gives $(\tau\sigma'_{fs})^{-1}$, while the intercept gives $(\sigma_{fs}+\sigma_{tr})/\sigma'_{fs}$ [see Eq. (7)]. To obtain σ'_{fs} from the gradient, we need the value of the radiative lifetime τ of the $nD_{5/2}$ state. Fortunately, some recent experimental measurements[23-25] of the $nD_{3/2}$ radiative lifetimes are available, as given in Table III, which we shall use to convert the gradient and intercept into σ'_{fs}, σ_{fs} and σ_{tr} [the relation between σ'_{fs} and σ_{fs} in Eq. (4) is also used]. We note that theoretically, lifetimes of the $nD_{3/2}$ and $nD_{5/2}$ states are nearly equal, so that we shall use the experimental lifetimes of the $nD_{3/2}$ states for τ in the present data analysis. The cross sections so obtained are listed in Table IV. These cross sections are constant in the temperature range of 140 to 200 °C. The uncertainty in σ'_{fs} and σ_{fs} is estimated as 20%, due to the uncertainties in the vapor pressure,[22] in the ratio $(A_{5/2}/A_{3/2})$ used in (8), and in τ listed in Table III (the statistical uncertainty is much smaller, typically ~5%); the uncertainty in σ_{tr} is typically 25% or larger, which is due both to the uncertainty in σ'_{fs} and in the extrapolation of the straight lines in Fig. 3 to zero $(Nv)^{-1}$. It should be noted that the present values of the cross sections depend on the rather uncertain values of $A_{5/2}/A_{3/2}$ and τ used, and the uncertainties of these values con-

TABLE III. Experimental radiative lifetimes τ used in the data analysis to convert the gradients in Fig. 3 into σ'_{fs}.

State	τ (nsec)	Authors
$6D$	68	Marek and Niemax (Ref. 23)
$7D_{3/2}$	98 ± 10	Marek (Ref. 24)
$8D_{3/2}$	152 ± 3	Deech *et al.* (Ref. 25)
$9D_{3/2}$	218 ± 4	Same
$10D_{3/2}$	311 ± 6	Same

TABLE IV. Experimental cross sections for fine-structure-changing collisions (σ'_{fs} and σ_{fs}) and for transfer out of the nD doublet (σ_{tr}) for collisions of Cs($nD_{3/2,5/2}$) with a ground state Cs atom. r^2 is the hydrogenic expectation value of the square of the orbit radius. All values are in units of 10^{-14} cm^2.

n	σ'_{fs} ($nD_{3/2} \rightarrow nD_{5/2}$)	σ_{fs} ($nD_{5/2} \rightarrow nD_{3/2}$)	σ_{tr} ($nD_{5/2} \rightarrow$ out of doublet)	r^2
6	2.7±0.5	2.1±0.4	1.1±0.6	0.8
7	3.7±0.7	2.7±0.5	5.3±1.5	2.5
8	8.6±1.7	6.0±1.2	3.6±1.5	5.8
9	18.4±3.7	12.6±2.7	6.3±2.3	11.8
10	29.8±6.0	20.2±4.0	15.5±4.0	21.2

stitute a major source of uncertainties in the cross sections. However, if better values of $A_{5/2}/A_{3/2}$ and τ become available in the future, then a better value of σ'_{fs} or σ_{fs} will be

$$(\sigma'_{fs})_{future} = \left(\sigma'_{fs}\frac{A_{5/2}}{A_{3/2}}\tau\right)_{now} \Big/ \left(\frac{A_{5/2}}{A_{3/2}}\tau\right)_{future}, \quad (9)$$

where quantities subscripted "now" are values given in the present paper, and quantities subscripted "future" are future improved values of the corresponding quantities. A better value of σ_{tr} will be given by

$$\left(\frac{\sigma_{fs}+\sigma_{tr}}{\sigma'_{fs}\,A_{5/2}/A_{3/2}}\right)_{now} = \left(\frac{\sigma_{fs}+\sigma_{tr}}{\sigma'_{fs}\,A_{5/2}/A_{3/2}}\right)_{future}. \quad (10)$$

IV. DISCUSSION

The higher-nD states studied in the present experiment have rather large orbits for the valence electron. An effective quantum number n^* for these states can be defined by

$$E_n = -(13.6/n^{*2})\ \text{eV}, \quad (11)$$

where E_n is the energy of the nD state measured from the ionization limit. Values of n^* for the states studied are listed in Table II. The hydrogenic expectation value of the square of the orbit radius is given by[26]

$$r^2 = \tfrac{1}{2}n^{*2}[5n^{*2}+1-3l(l+1)]a_0^2, \quad (12)$$

where $l=2$ for the nD states and a_0 is the Bohr radius. The calculated values of r^2, which is an approximate estimate of the geometrical cross section of the excited atom, are listed in Table IV. It is interesting to note that the fine-structure-changing cross sections for the $7D$–$10D$ states are nearly the geometrical cross sections:

$$\left.\begin{aligned}\sigma'_{fs} &\approx 1.5\,r^2\\ \sigma_{fs} &\approx 1.0\,r^2\end{aligned}\right\} \text{ for } n=7 \text{ to } 10. \quad (13)$$

The $6D$ state is a clear exception with an anomalously large σ'_{fs} and σ_{fs}.

Equations (12) and (13) indicate that σ'_{fs} and σ_{fs} vary nearly as n^{*4}, except for the $6D$ state. Indeed, $\pi n^{*4}a_0^2$ (a very rough estimate of the geometrical cross section) is found to be equal to σ_{fs}, within the uncertainty limits, for $n=7$–10. The n^{*4} dependence is shown clearly in Fig. 4, where the fine-structure-changing cross sections are plotted versus n^*. The straight lines have a gradient of n^{*4}. Recently, Deech *et al.*[25] measured the total depopulation cross section of

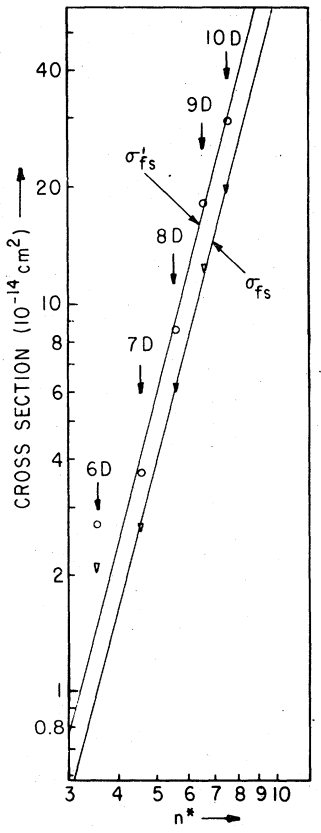

FIG. 4. Plot of the fine-structure-changing cross sections σ'_{fs} and σ_{fs} vs the effective quantum number n^*. The straight lines have a gradient of n^{*4}.

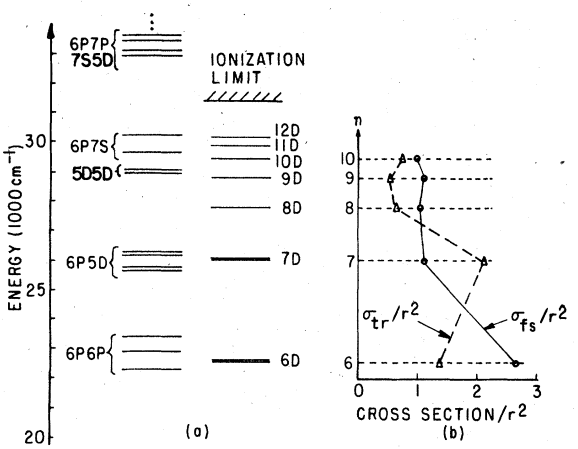

FIG. 5. (a) Energy levels of excited states of Cs. On the left-hand side are energies of two excited Cs atoms as indicated. On the right-hand side are energies of some nD states. Note that the $6D$ level is very near to the energy of two $6P$ atoms, and the $7D$ level is very near to the energy of a $6P$ atom plus a $5D$ atom. (b) Plot of the "reduced cross sections" [cross section/r^2] for the various nD states studied.

$Cs(n^2D_{3/2})$ atoms due to collisions with $Cs(6S)$ atoms for $n = 8$ to 14, and they also observed an n^{*4} dependence. Our data is consistent with their data, which is comparatively less accurate: e.g., the total depopulation cross section for $Cs(10D_{3/2})$ is quoted[25] as $(6 \pm 5) \times 10^{-13}$ cm^2.

A better understanding of the dependence of the cross sections on principal quantum numbers can be gained by plotting "reduced cross sections" σ/r^2 along with the term values of the D states and various final states to which the D states can be converted by collisions. Such a plot is shown in Fig. 5. It is interesting to note that there are two nearly resonant reactions

$$Cs(6D) + Cs(6S) \rightarrow Cs(6P) + Cs(6P) + 232\ \text{cm}^{-1} \tag{14}$$

and

$$Cs(7D) + Cs(6S) \rightarrow Cs(6P) + Cs(5D) - 163\ \text{cm}^{-1}. \tag{15}$$

The energy defects on the right-hand sides of (14) and (15) are the smallest values which can be obtained from various combinations of fine-structure sub-levels in (14) and (15). These energy defects are smaller than kT ($kT \lesssim 350$ cm^{-1}) for our experimental conditions, and we may expect (14) and (15) to have unusually large forward and reverse cross sections. This expectation is borne out by the large values of σ_{tr} for $6D$ and $7D$. The preferential excitation transfer collison (14) was studied in more detail in Ref. 13, and its cross section was estimated as $(1.5^{+1.5}_{-0.7}) \times 10^{-14}$ cm^2. However, the reaction corresponding to (15) for the $8D$ state,

$$Cs(8D) + Cs(6S) \rightarrow Cs(6P) + Cs(5D) + 1480\ \text{cm}^{-1}, \tag{16}$$

has an energy defect of 1480 cm^{-1} which is substantially larger than kT. In fact, $\sigma_{tr}(8D)$ is actually smaller than $\sigma_{tr}(7D)$ even though the geometrical cross section for the $8D$ state is more than twice as large as that of the $7D$ state (see Table IV). The anomalously large fine-structure mixing cross section $\sigma_{fs}(6D)$ is probably also due to the nearly resonant reaction (14). However, it seems that the proximity of doubly excited levels to an nD state is a necessary but not sufficient condition for large inelastic cross sections in the $Cs(nD) + Cs(6S)$ collision cross sections.

In conclusion, we have made the first measurements of the fine-structure-changing cross sections, and also measured the excitation-transfer cross sections of the nD states of an alkali-metal atom due to collisions. The cross sections observed in the present investigation for the case of self-collisions in Cs are found to be nearly equal to the geometrical cross sections for $n = 7$ to 10; in other words, every ground-state cesium atom which passes within a distance $\sim (n^*)^2 a_0$ of the excited atom $Cs^*(nD)$ causes a transition between fine-structure doublets or a transition out of the nD state. Such collisions, which involve a very spatially extended excited-state wave function cannot be completely described by a long-range dipole-dipole interaction of the Van der Waals type. Rather the slowly moving valence electron of the excited atom may be visualized as interacting with the relatively compact ground-state atoms which happen to be within the outer turning point of the orbit of the excited electron. Our measurements also show that the cross sections may be significantly enhanced when resonant reactions like (14) and (15) are possible (see Fig. 5). A comprehensive review of some methods to calculate cross sections of Rydberg atoms can be found in a recent article by Omont.[27] Because of the striking systematic trend of the D-state cross sections, which we have demonstrated in this paper, detailed calculations of these cross sections for the D states of cesium would be of considerable interest.

ACKNOWLEDGMENTS

This research was supported by the National Science Foundation under Grant No. NSF-ENG76-16424 and by the Joint Services Electronics Program under Contract No. DAAG29-77-C-0019. One of us (S.M.C.) would like to thank the Alfred P. Sloan Foundation for financial support.

*Present address: Bell Laboratories, Murray Hill, N.J. 07974.
†On leave from the Ionosphere Research Laboratory, Kyoto University, Kyoto, Japan.
‡On leave from the Univ. of Texas at Dallas, P.O. Box 688, Richardson, Tex. 75080.

[1]A. Gallagher, Phys. Rev. 172, 88 (1968).
[2]J. Cuvellier, P. R. Fournier, F. Gounard, J. Pascale, and J. Berlande, Phys. Rev. A 11, 846 (1975).
[3]L. Krause, Appl. Opt. 5, 1375 (1966).
[4]P. L. Lijnse *et al.*, J. Quant. Spectrosc. Radiat. Transfer 13, 1033 (1973); 13, 1301 (1973); 14, 1079 (1974); 14 1143 (1974); and 14, 1195 (1974).
[5]J. Callaway, Phys. Rev. A 140, 1072 (1966).
[6]F. Masnou-Seeuws, J. Phys. B 3, 1437 (1970).
[7]E. E. Nikitin and A. J. Reznikov, Chem. Phys. Lett. 8, 161 (1971).
[8]J. Pascale and P. M. Stone, J. Chem. Phys. 65, 5122 (1976).
[9]T. F. Gallagher *et al.*, Phys. Rev. Lett. 35, 644 (1975); Phys. Rev. 15, 1937; 15, 1945 (1977); 16, 441 (1977).
[10]S. G. Leslie, J. T. Verdeyen, and W. S. Millar, J. Appl. Phys. 48, 4444 (1977).
[11]C. Manus, Physica C 82, 165 (1976).
[12]J. Pascale and J. Vandeplanque, J. Chem. Phys. 60, 2278 (1974).
[13]T. Yabuzaki, A. C. Tam, M. Hou, W. Happer and S. M. Curry, Opt. Commun. 24, 305 (1978).
[14]C. B. Collins, B. W. Johnson, M. Y. Mirza, D. Popescu, and I. Popescu, Phys. Rev. A 10, 813 (1974).
[15]A. C. Tam and W. Happer, Opt. Commun. 21, 403 (1977).
[16]L. K. Lam, T. Fujimoto, A. C. Gallagher, and A. V. Phelps, Bull. Am. Phys. Soc. 22, 193 (1977).
[17]L. K. Lam, T. Fujimoto, A. C. Gallagher, and M. M. Hessell, J. Chem. Phys. (to be published).
[18]P. Tsekeris and W. Happer (unpublished).
[19]O. S. Heavens, J. Opt. Soc. Am. 51, 1058 (1961).
[20]P. M. Stone, Phys. Rev. 127, 1151 (1962).
[21]B. Warner, Mon. Not. R. Astr. Soc. 139, 115 (1968).
[22]A. N. Nesmeyanov, *Vapor Pressures of the Elements* (Academic, New York, 1963).
[23]J. Marek and K. Niemax, J. Phys. B 9, L483 (1976).
[24]J. Marek, Phys. Lett. 60A, 190 (1977).
[25]J. S. Deech, R. Luypaert, L. R. Pendrill, and G. W. Series, J. Phys. B 10, L137 (1977).
[26]H. Bethe and E. E. Salpeter, Handb. Phys. 35, 88 (1957).
[27]A. Omont, J. Phys. 38, 1343 (1977).